Supplementary Information to the manuscript having the title

Multitargeting Antibacterial Activity of a Synthesized Mn^{2+} Complex of Curcumin on Gram-Positive and Gram-Negative bacterial strains

[a]Tanmoy Saha[‡], [b]Prince Kumar[‡], [a]Nayim Sepay, [c]Durba Ganguly, [b]Kanchan Tiwari, [b]Kasturi Mukhopadhyay[*] and [a]Saurabh Das[*]

[a]Department of Chemistry (Inorganic Section), Jadavpur University, Kolkata – 700032, INDIA.
[b]School of Environmental Sciences, Jawaharlal Nehru University, New Delhi – 110067, INDIA.
[c]Department of Inorganic Chemistry, Indian Association for the Cultivation of Science, Kolkata – 700032, INDIA.

*** Corresponding author. Tel: +91 33 24572148; +91 33 8902087756**
Fax: +91 33 24146223
E-mail address: dasrsv@yahoo.in kasturim@mail.jnu.ac.in; kasturi26@hotmail.com

‡: TS & PK have equal contribution

Present address of Prince Kumar: Department of Botany, T. S. College, Hisua, Nawada, Magadh University, Bodhgaya – 824 234, India.

The supporting information for this manuscript includes

1) A figure (S1) showing the absorption spectra of Curcumin and the Mn^{II} complex in DMSO.
2) A figure (S2) showing absorption spectra of Mn^{II} interacting with Curcumin in ethanol-water as solvent during determination of stoichiometry of complex forimation.
3) A figure (S3) showing the infra-red spectrum of Curcumin .
4) A figure (S4) showing the infra-red spectrum of $[Mn^{II}(Cur)_2(HCur)]$.
5) A figure (S5) showing TGA of $[Mn^{II}(Cur)_2(HCur)]$.
6) A schematic diagram (S6) showing the keto-enol tautomerism of Curcumin.
7) A Table (S1) showing the optimized bond lengths for the carbon-oxygen bonds of Curcumin involved in coordination of Mn^{II}.
8) A figure (S7) showing degradation of Curcumin and no degradation of the complex as realized from a change in absorbance in the UV-visible region after being taken in PBS buffer or in PBS buffer with 10 μM DTT.
9) A figure (S8) showing degradation of Curcumin and no degradation of the complex realized from a change in absorbance in the UV-visible region after being taken in different bacterial growth medium.
10) Double reciprocal plot for interaction of $[Mn^{II}(Cur)_2(HCur)]$ with calf thymus DNA. using UV-Vis spectroscopy (Fig. S9).
11) Double reciprocal plot with y intercept = 1 for interaction of $[Mn^{II}(Cur)_2(HCur)]$ with calf thymus DNA using UV-Vis spectroscopy (Fig. S10).
12) A figure (S11) showing bacterial survival in logarithmic scale to indicate antibacterial efficacy of $[Mn^{II}(Cur)_2(HCur)]$ and Curcumin on *S. aureus* and *E. coli* cells.
13) A figure (S12) showing scanning electron microscope images of *S. aureus* ATCC 29213 treated with either no compound or with Curcumin, $[Mn^{II}(Cur)_2(HCur)]$ and gramicidin D to realize membrane permeabilization of *S. aureus* by the calcein leakage assay.
14) Equations related to the dissociation of the three protons on Curcumin.
15) A figure (S13) showing the spectrophometric titration of Curcumin followed at 467 nm.
16) Figures showing mole ratio plots (S14A & S14B) and Job's plots of continuous variation (S14C) for Curcumin with Mn^{II} that were followed at 430 nm.

17) A figure (S15) showing the spectrophometric titration of Curcumin in the presence of Mn^{II} followed at 430 nm.

18) Equations for the evaluation of stability constant of the complex formed in solution based on the interaction of HCur with Mn^{II} by evaluation of pK_a values of HCur in the absence and presence of Mn^{II}.

Figure S1

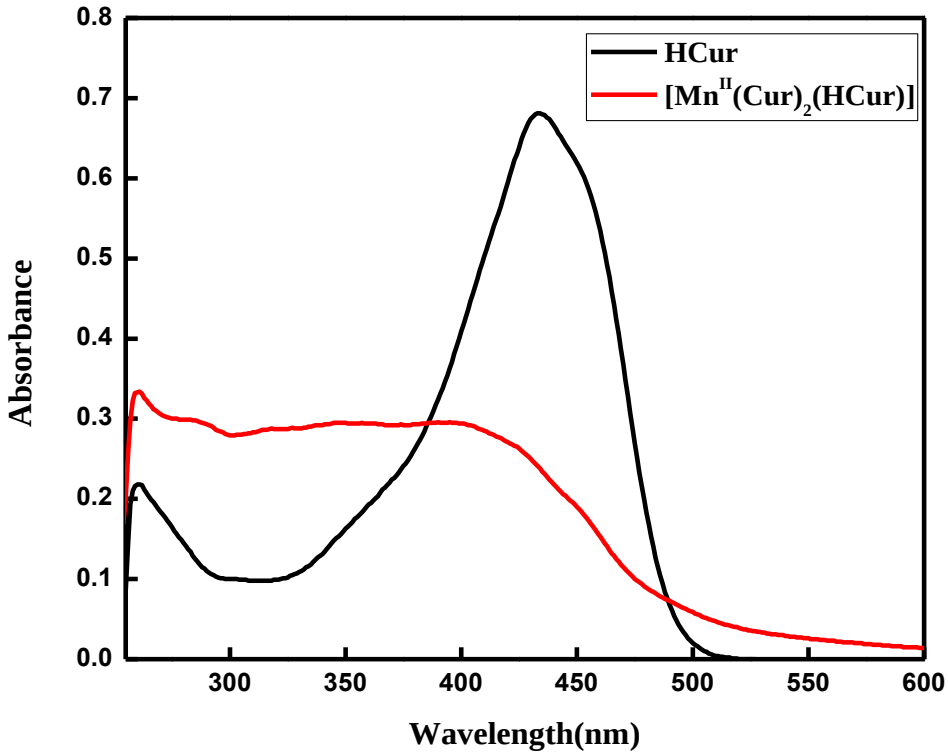

Figure S1: Absorption spectra for HCur and $[Mn^{II}(Cur)_2(HCur)]$ in DMSO.

Figure S2

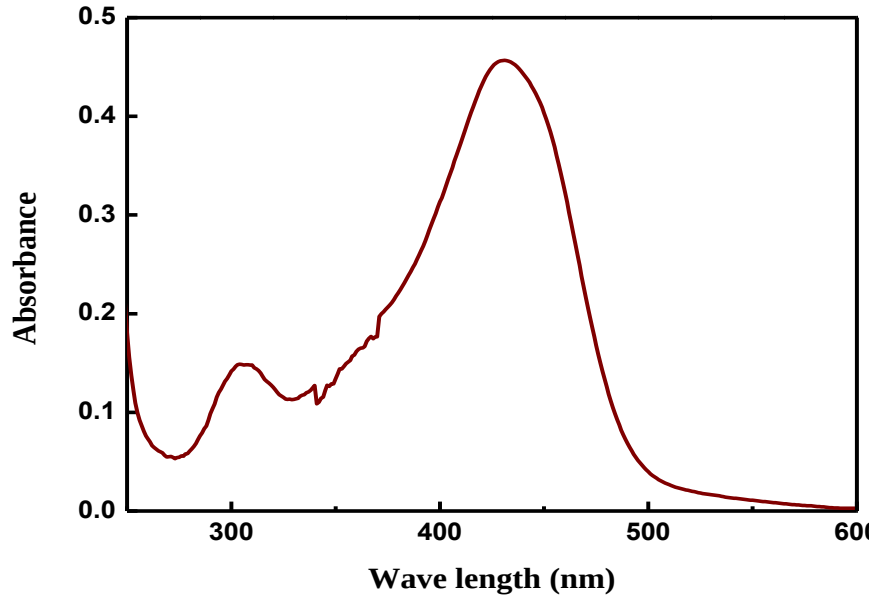

Figure S2: Absorption spectra for Mn^{II} interacting with Curcumin in ethanol-water during a stoichiometry determination experiment.

Figure S3

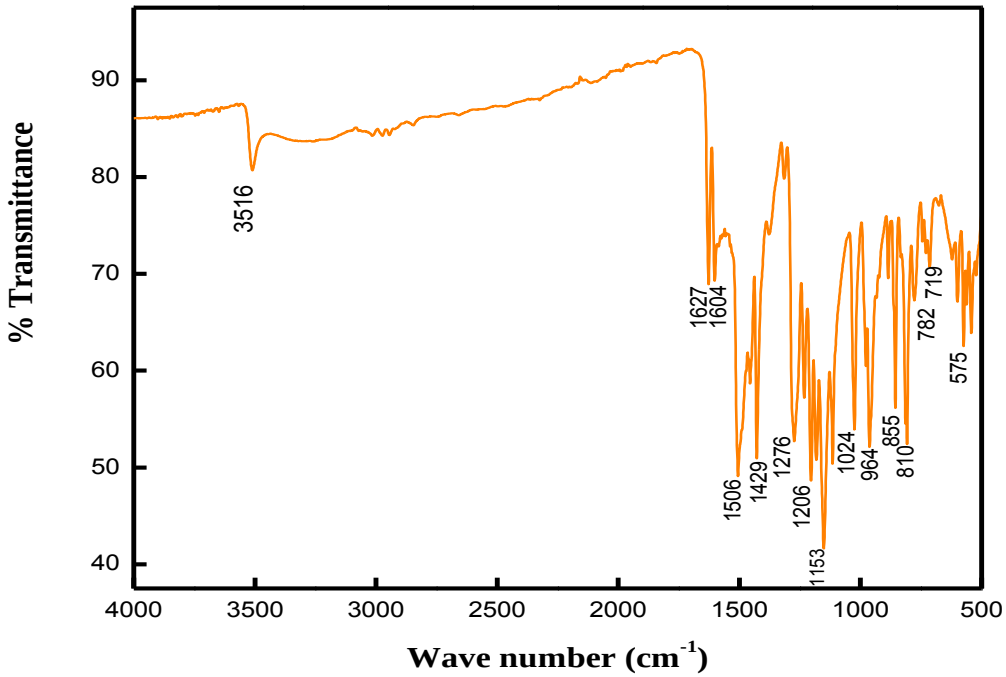

Figure S3: FTIR spectrum of HCur

Figure S4

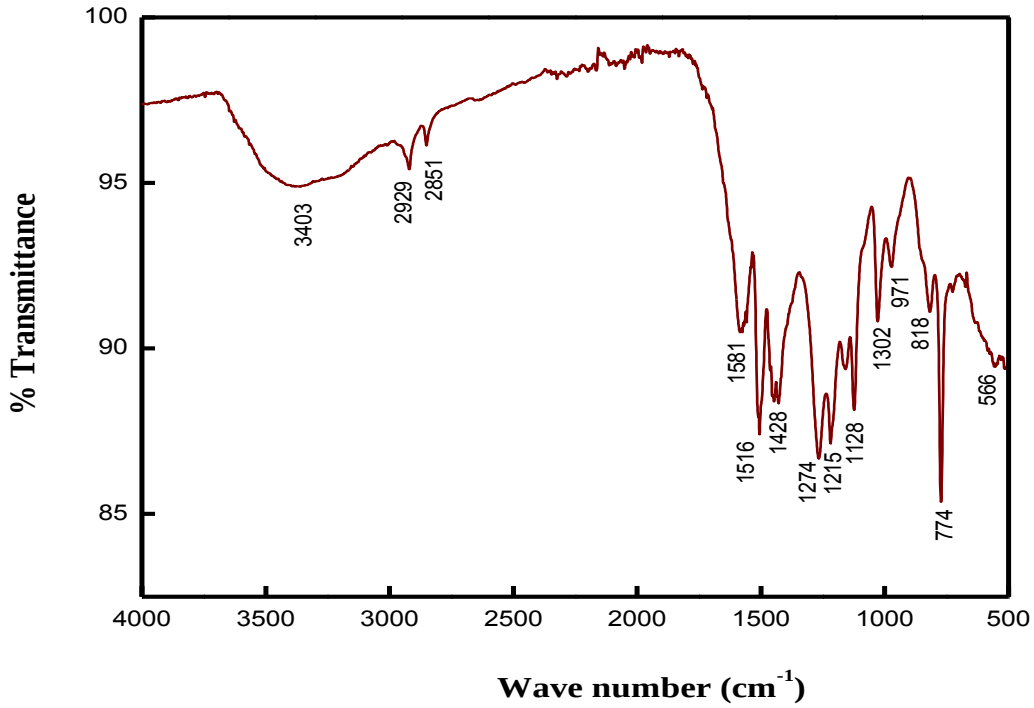

Figure S4: FTIR spectrum for $[Mn^{II}(Cur)_2(HCur)]$

Figure S5

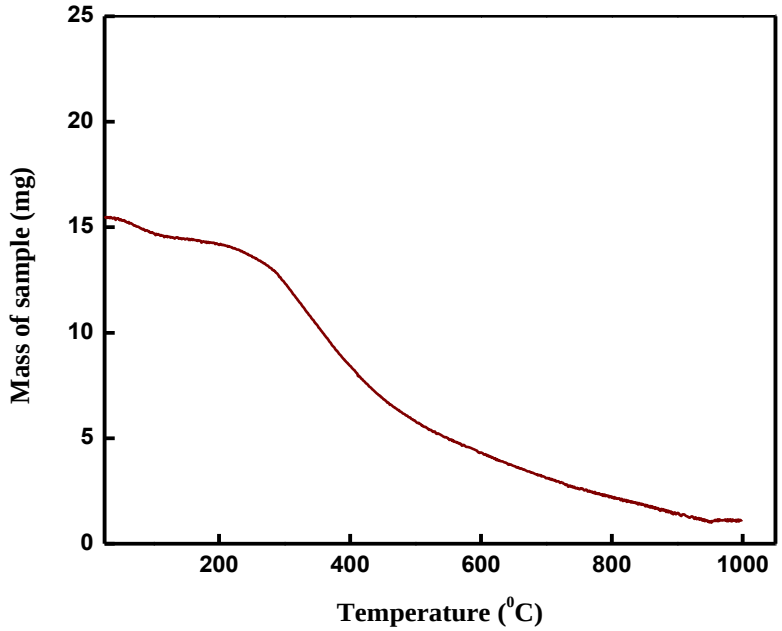

Figure S5: TGA of $[Mn^{II}(Cur)_2(HCur)]$

Figure S6

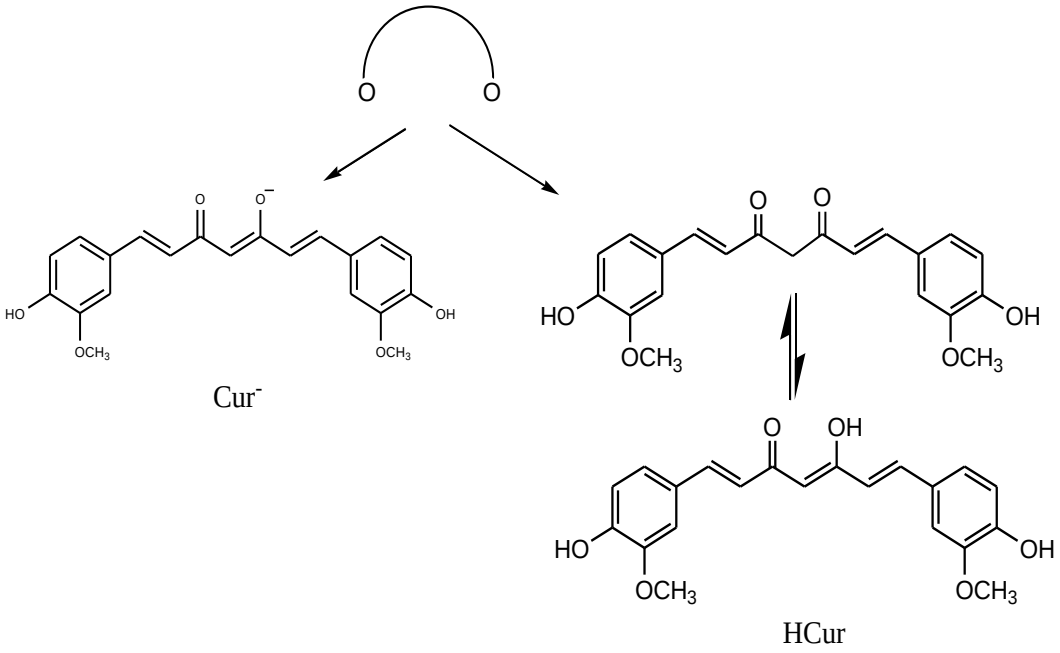

Figure S6: Structures of Curcumin in the diketo and enolate anion forms.

Table S1: Optimized bond lengths for carbon-oxygen bonds of Curcumin involved in coordination of Mn^{II}.

Bond Type	Bond Length (Å)
C16-O2	1.3051
C17-O4	1.3001
C15-O6	1.3193
C12-O5	1.3099
C11-O3	1.3101
C8-O7	1.3096

Figure S7

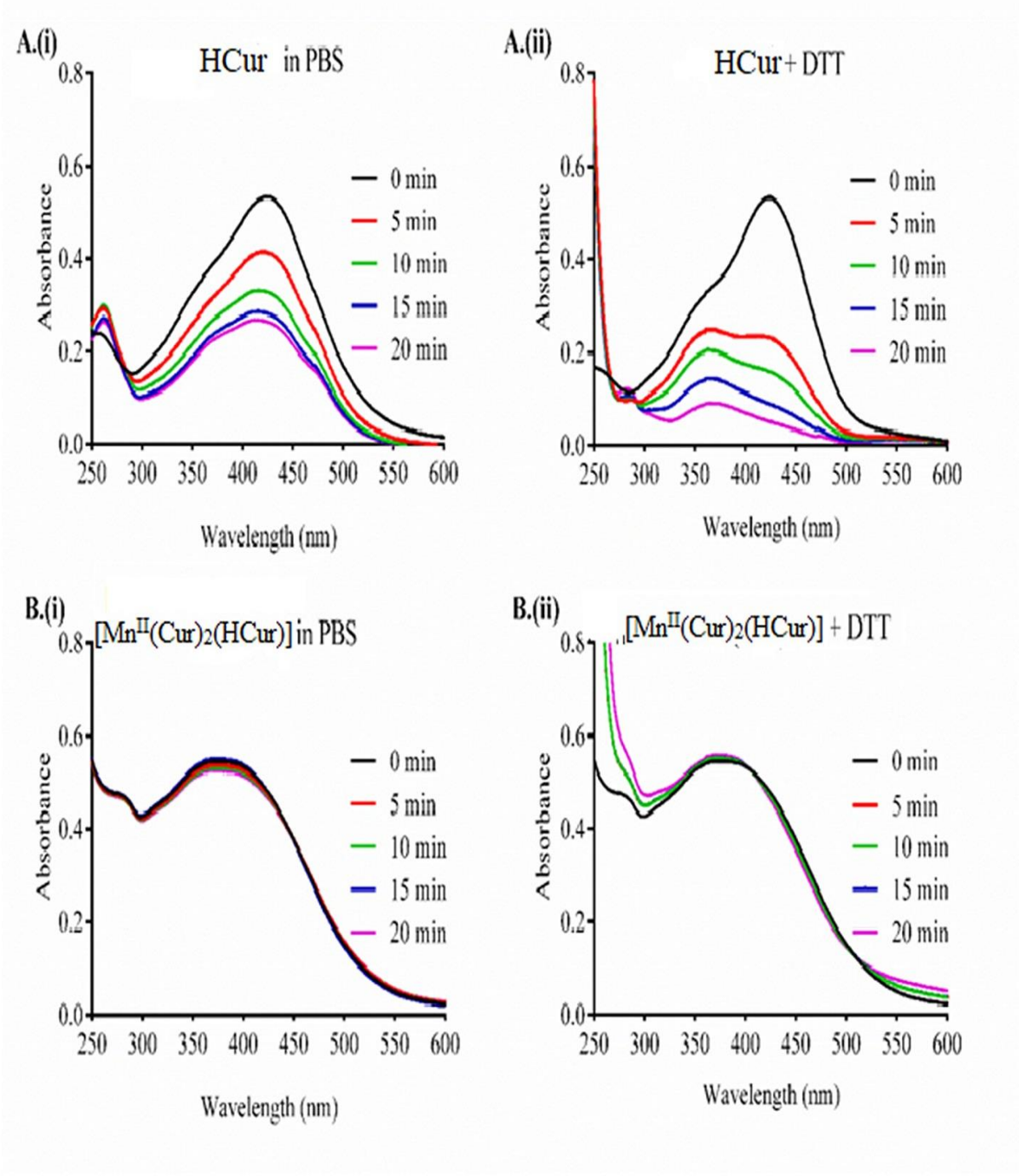

Figure S7: UV-visible spectra of (A) HCur and (B) [Mn^{II}(Cur)$_2$(HCur)] in presence of (i) only PBS buffer (pH 7.4) and (ii) PBS buffer with 10 µM DTT.

Figure S8

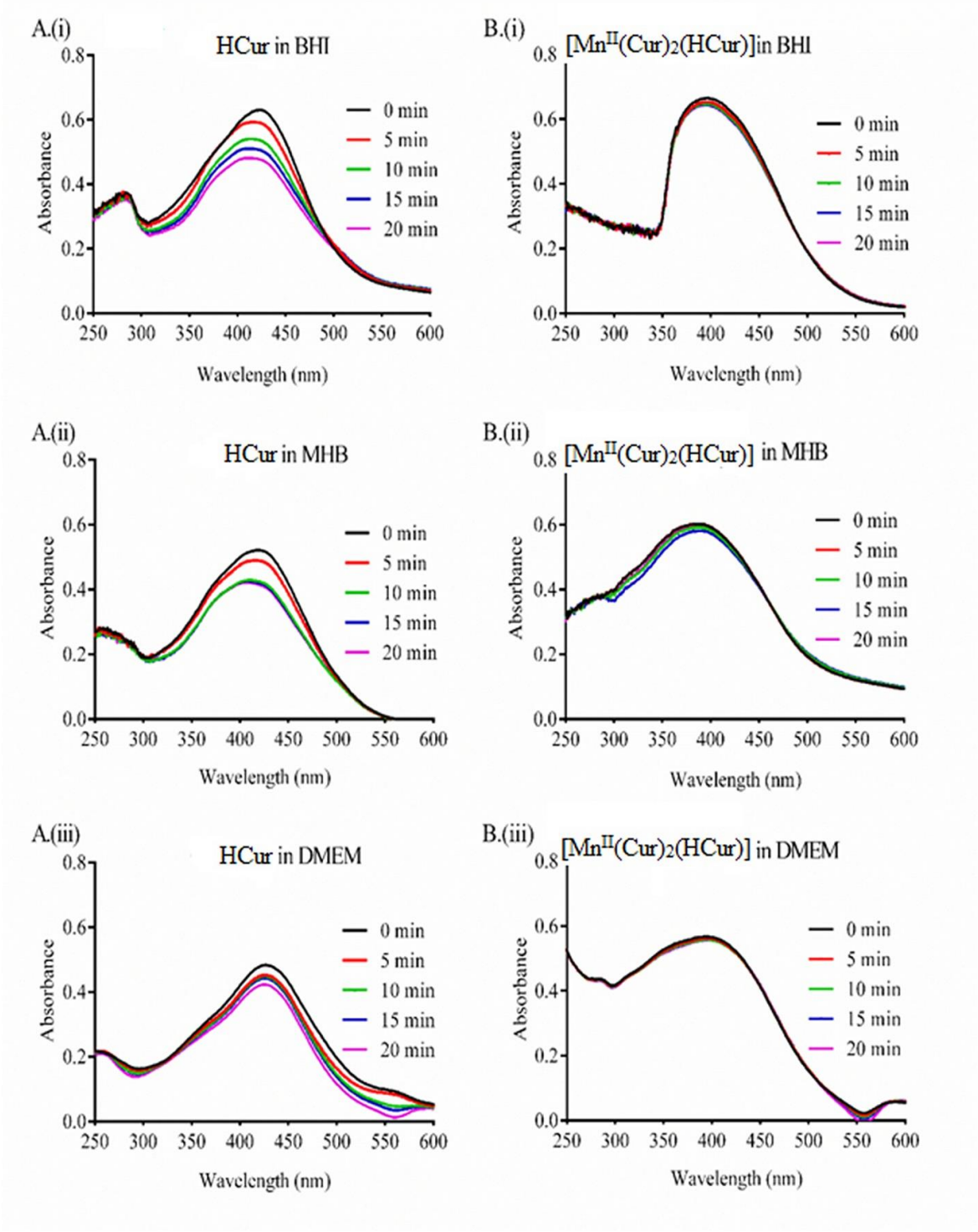

Figure S8: UV-visible absorption spectra of (A) HCur and (B) [Mn^{II}(Cur)$_2$(HCur)] in different bacterial growth medium (i) BHI, (ii) MHB, and (iii) DMEM.

Figure S9

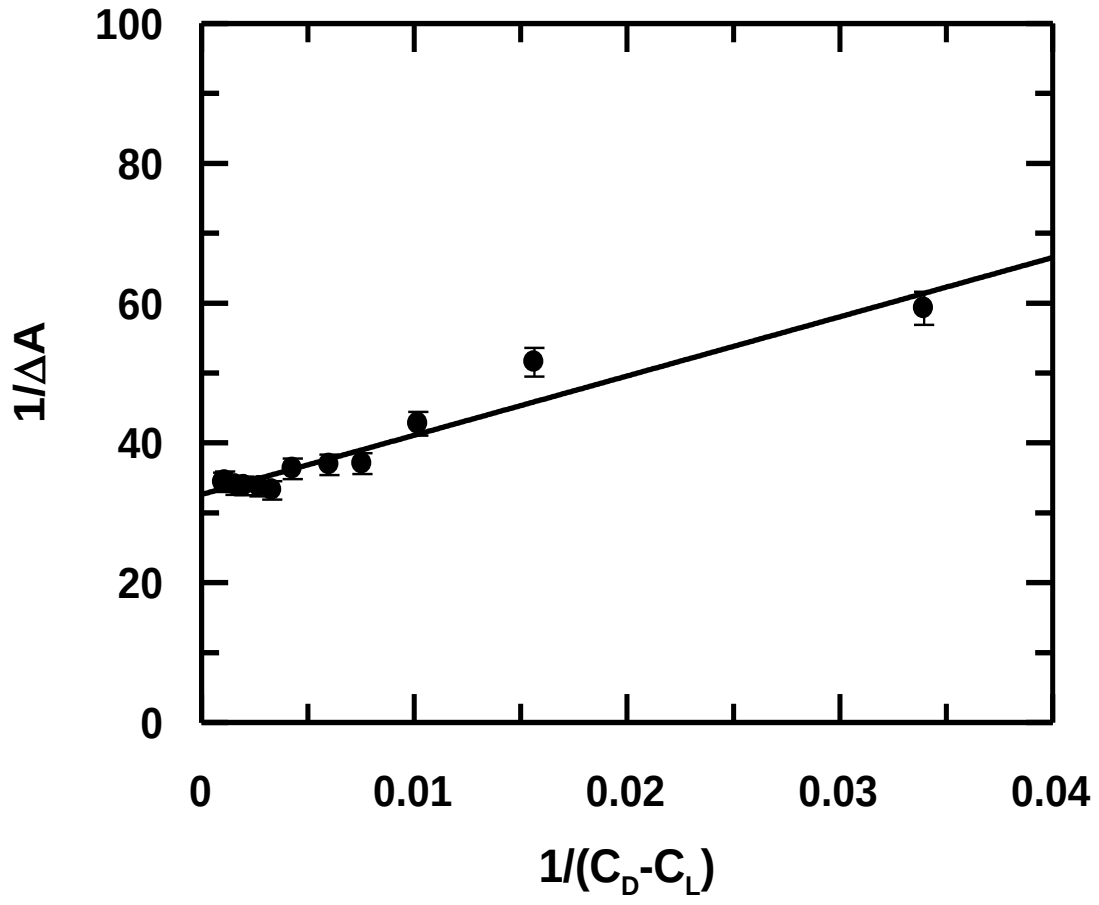

Figure S9: A double reciprocal plot for the interaction of $[Mn^{II}(Cur)_2(HCur)]$ with calf thymus DNA leading to the determination of apparent binding constant (K_{app}) at pH 7.4 (30 mM phosphate buffer) and ionic strength 0.15 M; $[Mn^{II}(Cur)_2(HCur)]$ = 40 µM, pH = 7.4; Temperature = 298 K.

Figure S10

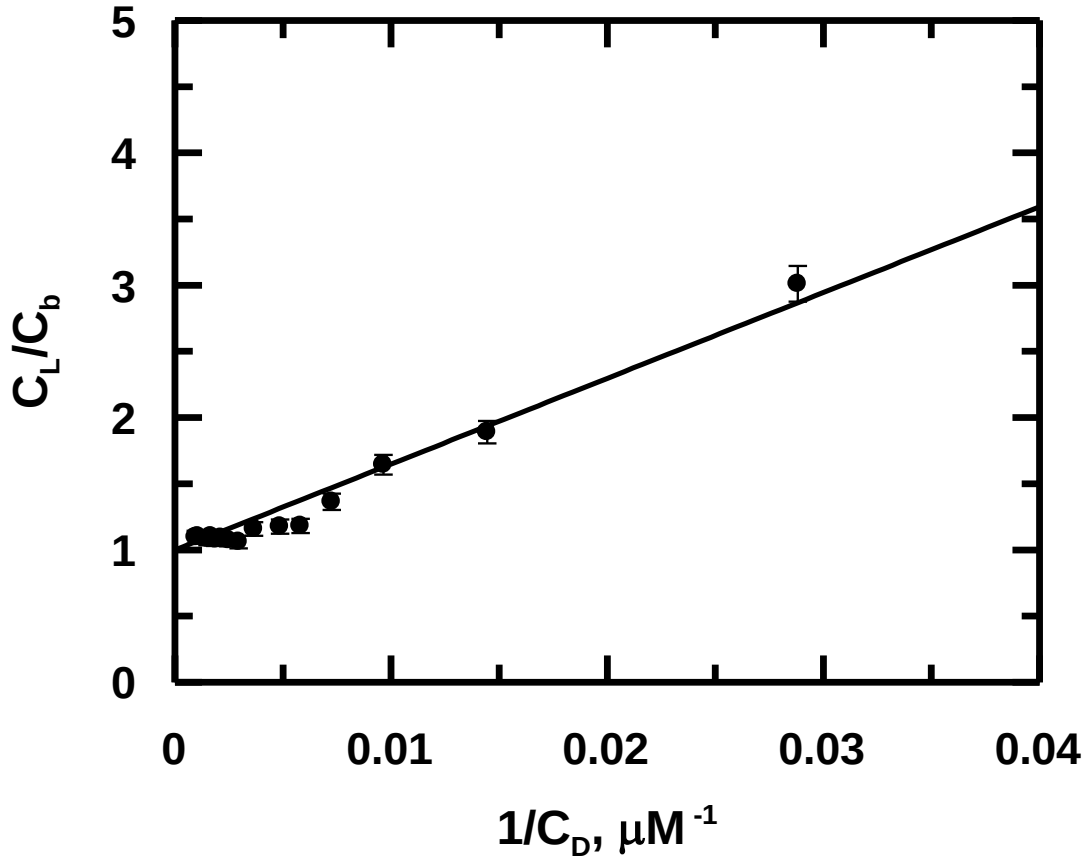

Figure S10: Double reciprocal plot for a UV-Vis titration of 40 μM [$Mn^{II}(Cur)_2(HCur)$] by calf thymus DNA using phosphate buffer (~pH 7.4) at 298 K.

Figure S11

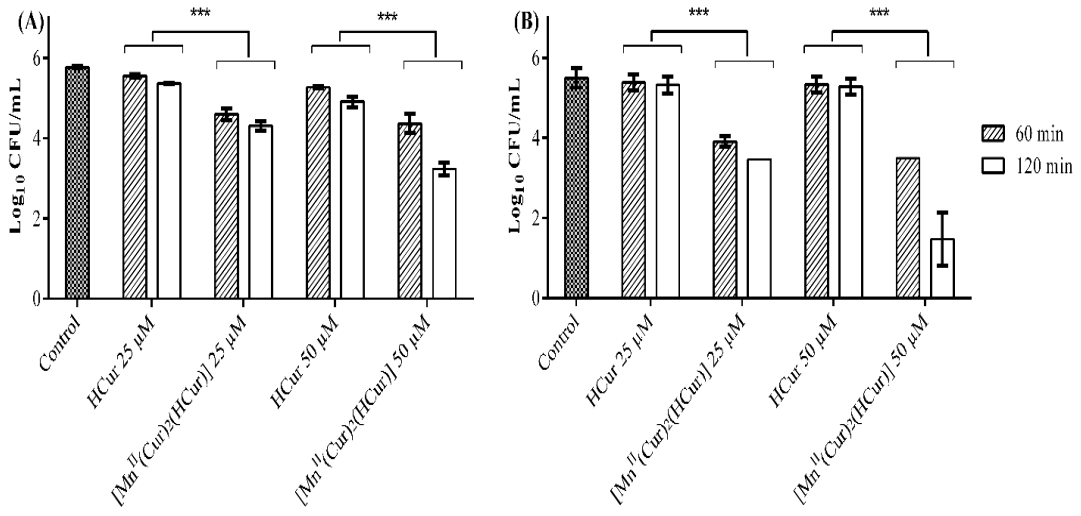

Figure S11: Antibacterial efficacy of 25 and 50 µM of $[Mn^{II}(Cur)_2(HCur)]$ and HCur in PBS buffer against (A) *S. aureus* and (B) *E. coli* cells (10^6 CFU/mL). Grey columns, columns with stripes, and white columns denote the time of exposure (2 min, 60 min, and 120 min, respectively) to the compounds. The data represent mean (± SD) of three independent experiments (* $p \leq 0.001$).**

Figure S12

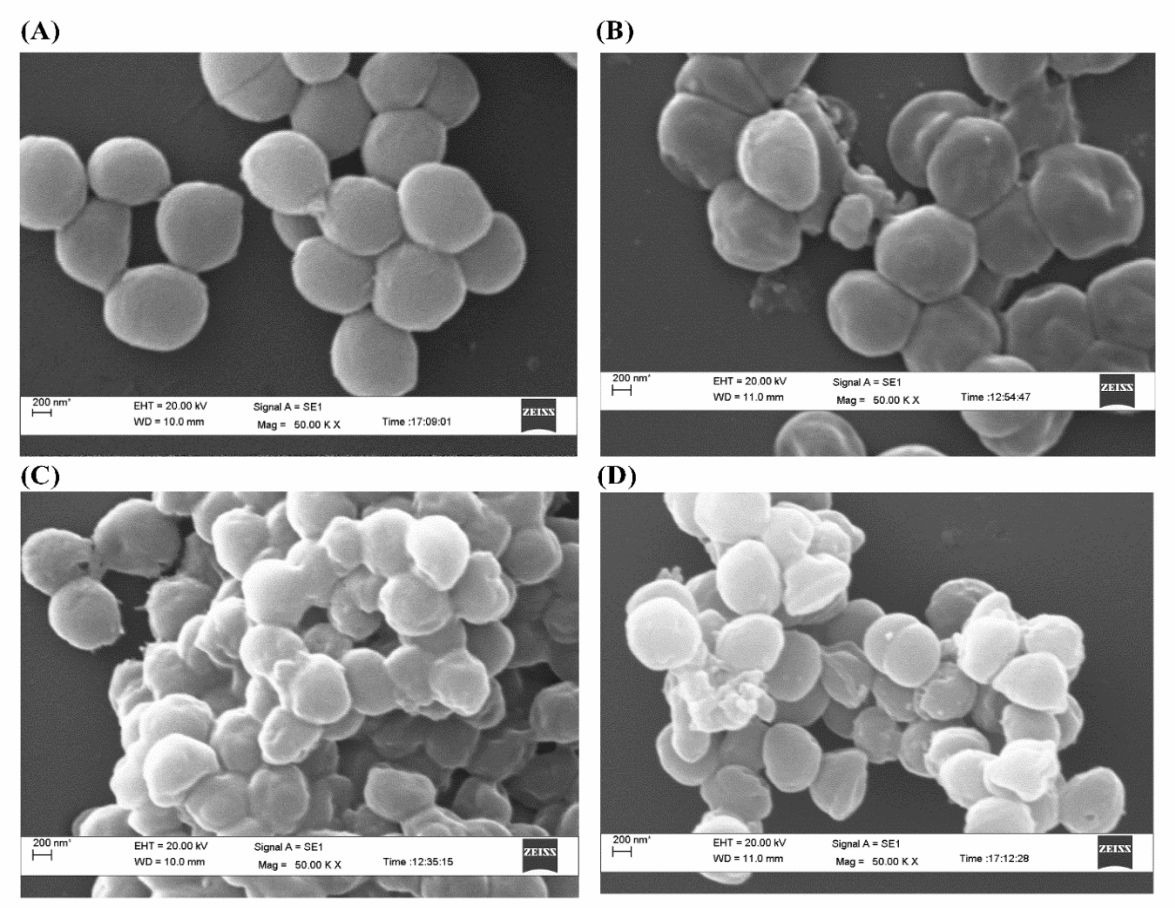

Figure S12: Scanning electron microscope images of *S. aureus* ATCC 29213 treated with 50 µM of HCur, $[Mn^{II}(Cur)_2(HCur)]$, and 20 µg/mL gramicidin D for 2 hours. (A) Untreated control cells, (B) HCur, (C) $[Mn^{II}(Cur)_2(HCur)]$ and (D) gramicidin D treated cells.

Equations with regard to the dissociation of the three protons on HCur.

$$LH_2H^* \rightleftharpoons LH_2^- + H^{*+} \quad K_1 = \frac{[H^{*+}][LH_2^-]}{[LH_2H^*]} \qquad (S1)$$

$$LH_2^- \rightleftharpoons L^{3-} + 2H^+ \quad K_2 = \frac{[L^{3-}][H^+]^2}{[LH_2^-]} \qquad (S2)$$

Figure S13

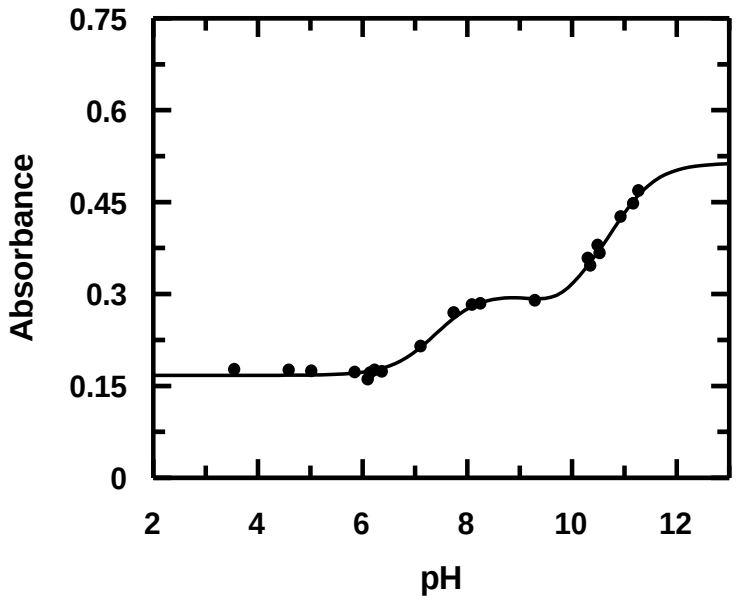

Figure S13: Spectrophotometric titration of HCur as shown by a variation in absorbance at 467 nm; [HCur] = 5 µM, [$NaNO_3$] = 0.1 M, Temperature =305K.

The change in absorbance of HCur at 467 nm was fitted to Eq. S3

$$A_{obs} = \frac{A_1}{(1 + 10^{pH - pKa1} + 10^{pH - pKa2} + 10^{pH - pKa3})} + \frac{A_2}{(1 + 10^{pKa1 - pH} + 10^{pH - pKa2}) + 10^{pH - pKa3}} +$$

$$\frac{A_3}{(1 + 10^{pKa1 - pH} + 10^{pKa2 - pH} + 10^{pH - pKa3})} + \frac{A_4}{(1 + 10^{pKa1 - pH} + 10^{pKa2 - pH} + 10^{pKa3 - pH})} \qquad (S3)$$

A_1, A_2, A_3 and A_4 refer to absorbance due to LH_2H^*, LH_2^-, $LH^{2-}$and L^{3-} respectively while pK_{a1}, pK_{a2}, pK_{a3} are pK_a values for the dissociation of three protons on Curcumin (Eqs. S1 and S2).

Experiments to determine stoichiometry of complex formation:

In experiments for mole-ratio and Job's method of continuous variation appropriate amounts of HCur was mixed with Mn(II) in 10 mL volumetric flasks and after shaking the solution for a constant time of 3 minutes, absorbance was recorded. This was then plotted for all the three types of experiments.

If we consider the metal ion to be M and ligand L, then for our case since there is the formation of a 1:3 metal to ligand complex, sequence of reactions would be

$$M + L \leftrightarrows ML \quad (1)$$

$$ML + L \leftrightarrows ML_2 \quad (2)$$

$$ML_2 + L \leftrightarrows ML_3 \quad (3)$$

Since each step is an equilibrium step and we are allowing only 3 minutes of shaking time before recording the absorbance using a spectrophotometer it is only likely that for each solution having a certain composition, all species (ML, ML_2 and ML_3) would be present simultaneously. If attainment of equilibrium 1 is fast and other two relatively slow, we should see responses for ML_2 and ML_3. However, if equilibrium 1 is slow we would see responses for ML and ML_2. Sometimes in such cases, we may not see an exclusive response for ML_3 in the time-frame of our analysis but rather the existence of two species say ML_2 and ML_3. However, if one refluxes M and L, taking L in excess, for say 4 to 5 hours, which we did in order to prepare the complex one may get ML_3 exclusively.

Something like this happened for Mn(II)-Curcumin where we got responses both from mole-ratio and Job's plots for species in between 1:2 and 1:3 (but tending to 1:3). Had equilibrium for

reaction 3 been fast we would have got a response for ML_3 only but probably that was not the case. In the course of our study, when we refluxed Mn(II) and Curcumin for 4 hours, to prepare the complex we obtained a 1:3 Mn(II)-Curcumin complex that provided a moleculat ion peak in mass spectrometry corresponding to the molecular weight of a 1:3 species. Here we are providing all figures related to such experiments leading to determination of stoichiometry.

Mole ratio plots where concentration of Curcumin was constant, Mn(II) varied:

1: Absorbance recorded immediately i.e. after mixing for 3 minutes

2: Absorbance recorded after 6 hours from mixing.

3: Absorbance recorded after 24 hours from mixing.

Figure S14A

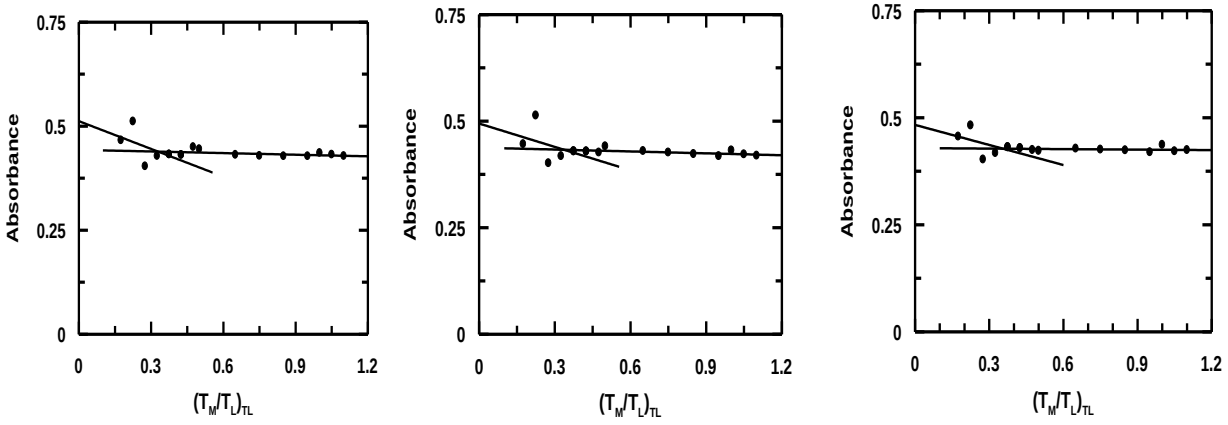

Figure S14A: Mole-ratio plots showing variation in absorbance at 430 nm for a change in concentration of Mn^{II} for a fixed concentration of HCur = 10 µM; (1) immediately after HCur and Mn(II) were mixed; (2) after 6 hours from the time HCur and Mn(II) were mixed; (3) after 24 hours from the time HCur and Mn(II) were mixed; pH of the medium: ~7.4, [$NaNO_3$] = 0.01 M, Temperature = 303 K.

Mole ratio plots where concentration of Mn(II) constant, Curcumin was varied:

1: Absorbance recorded immediately i.e. after mixing for 3 minutes

2: Absorbance recorded after 24 hours.

Figure S14B

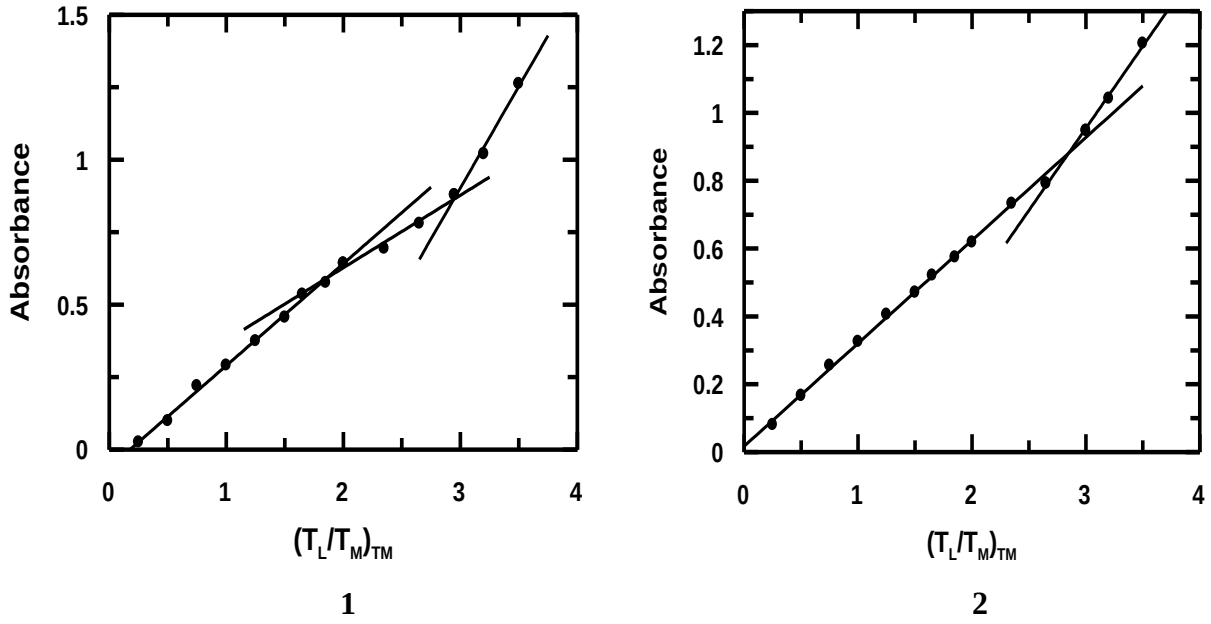

Figure S14B: Mole-ratio plots showing variation in absorbance at 430 nm for a change in concentration of HCur for a fixed concentration of Mn^{II} = 10 µM; (1) immediately after HCur and Mn(II) were mixed; (2) after 24 hours from the time HCur and Mn(II) were mixed; pH of the medium: ~7.4, [$NaNO_3$] = 0.01 M, Temperature = 303 K.

Job's plots from three separate experiments where both Mn(II) and Curcumin were varied continuously

Figure S14C

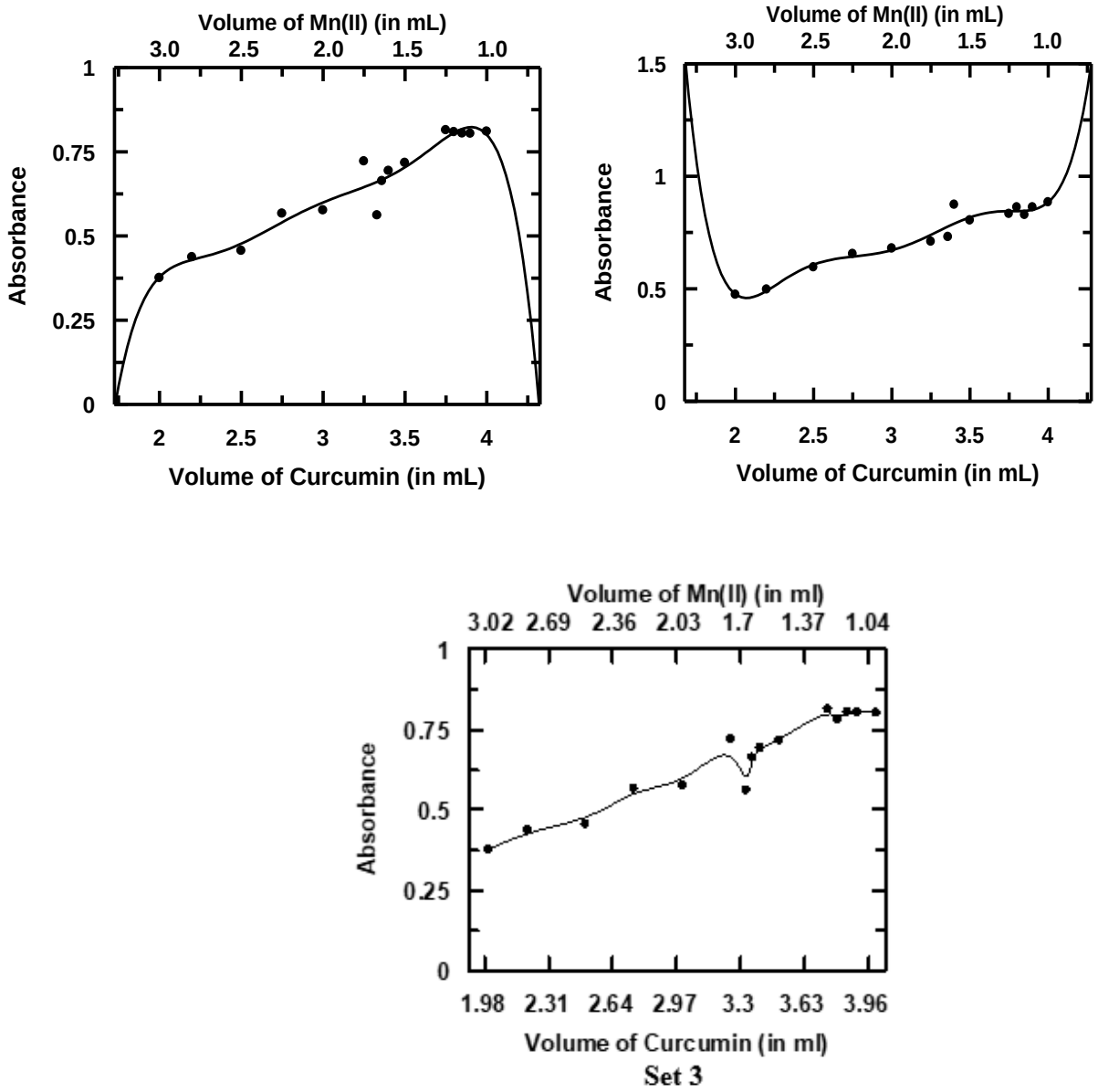

Figure. S14C: Plot showing a variation in absorbance at 430 nm for a continuous variation of HCur and Mn^{II} for three different experimental sets, Set 1, Set 2 and Set3 at pH (~7.4). Strength of stock solutions of Mn^{II} and HCur were 100 µM; [$NaNO_3$] = 0.01 M, Temperature = 303 K.

Figure S15

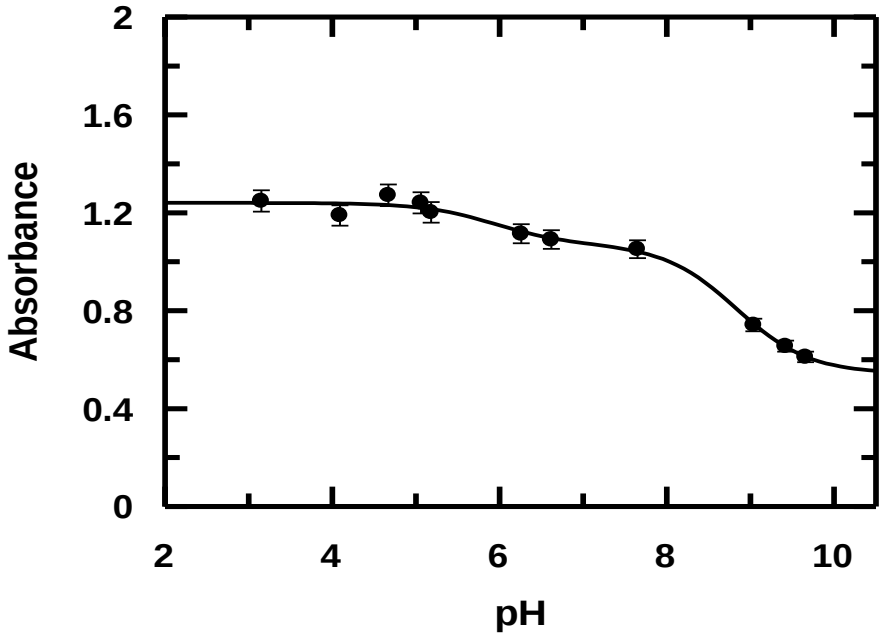

Figure S15: Titration of HCur performed in the presence of Mn^{II}, as shown by a variation in absorbance at 430 nm;[HCur] =30 µM, [Mn^{II}] = 10 µM, [$NaNO_3$] = 0.01 M, Temperature = 305 K.

$$A_{obs} = \frac{A_1}{(1 + 10^{pH - pKa1} + 10^{pH - pKa2})} + \frac{A_2}{(1 + 10^{pKa1 - pH} + 10^{pH - pKa2})} + \frac{A_3}{(1 + 10^{pKa1 - pH} + 10^{pKa2 - pH})} \quad (S4)$$

A_1, A_2 and A_3 are absorbances due to LH_2H^*, LH_2^- and L^{2-} respectively in the presence of Mn^{II}.

$$Mn^{2+} + 3LH_2H^* \rightleftharpoons [Mn(LH_2)_3]^- + 3H^{*+} \quad (S5)$$

$$\beta^* = \frac{[Mn(LH_2)_3][H^{*+}]^3}{[Mn^{2+}][LH_2H^*]^3} \quad (S6)$$

$$\text{or,} \quad Mn^{2+} + 3LH_2^- \rightleftharpoons [Mn(LH_2)_3]^- \quad (S7)$$

$$\beta = \frac{[Mn(LH_2)_3]}{[Mn^{2+}][LH_2^-]^3} \quad (S8)$$

$$\beta = \frac{\beta^*}{K_1^3} \quad (S9)$$

LH_2H^* represents HCur; K_1 is the dissociation constant of the enolic-OH proton of HCur.